Classical and Quantum Gravity

PAPER • **OPEN ACCESS**

Analytic solutions for parallel transport along generic bound geodesics in Kerr spacetime

To cite this article: Maarten van de Meent 2020 *Class. Quantum Grav.* **37** 145007

View the article online for updates and enhancements.

IOP ebooks™

Bringing together innovative digital publishing with leading authors from the global scientific community.

Start exploring the collection–download the first chapter of every title for free.

This content was downloaded from IP address 194.94.224.254 on 23/07/2020 at 08:55

OPEN ACCESS
IOP Publishing
Classical and Quantum Gravity
Class. Quantum Grav. **37** (2020) 145007 (16pp)
https://doi.org/10.1088/1361-6382/ab79d5

Analytic solutions for parallel transport along generic bound geodesics in Kerr spacetime

Maarten van de Meent

Max Planck Institute for Gravitational Physics (Albert Einstein Institute), Potsdam-Golm, Germany

E-mail: mmeent@aei.mpg.de

Received 27 August 2019, revised 18 February 2020
Accepted for publication 25 February 2020
Published 25 June 2020

Abstract

We provide analytical closed form solutions for the parallel transport along a bound geodesic in Kerr spacetime. This can be considered the lowest order approximation for the motion of a spinning black hole in an extreme mass-ratio inspiral. As an illustration of the usefulness of our new found expressions we scope out the locations of spin–spin resonances in quasi-circular EMRIs. All solutions are given as functions of Mino time, which facilitates the decoupling of the equations of motion. To help physical interpretation, we also provide an analytical expression for the proper time along a geodesic as a function of Mino time.

Keywords: Kerr black hole, analytic solutions, parallel transport, bound orbits

(Some figures may appear in colour only in the online journal)

1. Introduction

The motion of a freely falling frame in general relativity is described by the parallel transport of a frame along a geodesic. This is sometimes also referred to as the motion of a test gyroscope, i.e. a test particle that carries not only a position but also an orientation.

One situation where this becomes of interests is when a small spinning black hole orbits a much larger (possibly also spinning) black hole. Such systems—known as extreme mass-ratio inspirals—occur naturally in the centers of galaxies when a stellar mass black hole is captured by a supermassive black hole, and form a key potential source of gravitational waves for future space-based gravitational wave observatories such as LISA.

Original content from this work may be used under the terms of the Creative Commons Attribution 4.0 licence. Any further distribution of this work must maintain attribution to the author(s) and the title of the work, journal citation and DOI.

To first approximation—ignoring all effects due to its own mass and spin—the motion of a smaller (secondary) black hole is described by the parallel transport of its spin along a (bound) geodesic in the Kerr spacetime. As long as the spin of the primary is aligned with the total angular momentum of the system, the solution is fairly simple; the test object will follow an equatorial geodesic, and the spin will precess around the plane spanned by the four-velocity and total angular momentum.

Beyond this one can include the effects of the secondary's mass and spin order-by-order. The corrections to the trajectory are governed by the gravitational self-force (see [1] for a recent review and references), and Mathisson–Papatrou–Dixon force generated by the secondary spin (see [2–5] for some recent efforts at including its effects).

In this work we are interested in the motion of the secondary spin. In recent years it has become possible to calculate the correction to the precession rate of the secondary's spin linear in the secondary's mass. First for circular orbits around non-spinning black holes [6–10], and later extended to eccentric orbits [11–13], and spinning-black holes [14, 15].

Most of these efforts have restricted themselves to the 'easy' case where the spin of the primary is aligned with the total angular momentum. One reason for this is the lack of easily applicable closed form solutions for the parallel transport along a generic orbit. The purpose of this work is to fill this gap.

An elegant procedure for solving the parallel transport equations along a geodesic in Kerr spacetime was set out by Marck [16] in 1983. (With in recent years some clarifications being added by Bini and collaborators [17, 18].) This procedure effectively reduces the parallel transport equations to a single differential equation for the precession angle given a solution for the geodesic equation.

Closed form analytic solutions for bound geodesics in Kerr spacetime were derived by Fujita and Hikida [19] in 2009. This paper takes their method an extends it to a solution for Marck's equation for parallel transport.

The plan of this paper is as follows. In section 2 we review the analytic solution for bound geodesics found by Fujita and Hikida [19]. Along the way we establish most of the conventions and notations that we will need later. We also repackage the solutions of [19] in a much more compact and easier to use form. Section 3 then introduces Marck's formalism for solving the parallel transport equations, and gives analytical solutions following the procedures of [19]. In section 4 we illustrate the usefulness of our new found expressions by scoping out the locations of spin–spin resonances in quasi-circular EMRIs. As a bonus result, appendix C gives the analytical solution of the evolution of proper time as a function of Mino time along a geodesic.

The equations in this paper are given in geometric units such that $G = c = 1$. Appendix B establishes our conventions for elliptic functions.

2. Geodesic equations

The metric for a Kerr black hole of unit mass ($M = 1$) and spin a in (modified) Boyer–Lindquist coordinates is given by

$$\begin{aligned} \mathrm{d}s^2 = &-\left(1-\frac{2r}{\Sigma}\right)\mathrm{d}t^2 + \frac{\Sigma}{\Delta}\mathrm{d}r^2 + \frac{\Sigma}{1-z^2}\mathrm{d}z^2 + \frac{1-z^2}{\Sigma}\left(2a^2r(1-z^2)\right. \\ &\left. + (a^2+r^2)\Sigma\right)\mathrm{d}\phi^2 - \frac{4ar(1-z^2)}{\Sigma}\mathrm{d}t\,\mathrm{d}\phi, \end{aligned} \tag{1}$$

where z is related to the usual polar Boyer–Lindquist coordinate θ by $z = \cos\theta$. Furthermore,

$$\Delta := r(r-2) + a^2 \tag{2}$$

$$= (r - r_+)(r - r_-), \tag{3}$$

and

$$\Sigma := r^2 + a^2 z^2. \tag{4}$$

The locations of the inner and outer event horizon are denoted,

$$r_\pm = 1 \pm \sqrt{1 - a^2}. \tag{5}$$

Solving the geodesic equations is aided by the existence of four constants of motion. The first is given by the norm of the 4-velocity u^μ, which is set to -1 by the normalization of the proper time τ. The second and third are the (specific) energy $\mathcal{E}$ and angular momentum $\mathcal{L}$, given by the time translation and rotational Killing symmetries of Kerr spacetime,

$$\mathcal{E} := -u^\mu g_{\mu\nu} \left(\frac{\partial}{\partial t}\right)^\nu, \tag{6}$$

and

$$\mathcal{L} := u^\mu g_{\mu\nu} \left(\frac{\partial}{\partial \phi}\right)^\nu. \tag{7}$$

Finally, Carter [20] showed that there exist a fourth constant of motion, Q, related to the existence of a Killing tensor $\mathcal{K}_{\mu\nu}$, which (given as the 'square' of the Killing–Yano tensor $\mathcal{F}$) reads,

$$\mathcal{K}_{\mu\nu} := \mathcal{F}_{\mu\alpha}\mathcal{F}^\alpha{}_\nu, \tag{8}$$

where

$$\mathcal{F} := 2az\,\mathrm{d}r \wedge \left(\mathrm{d}t - a(1-z^2)\,\mathrm{d}\phi\right) + 2ar\,\mathrm{d}z \wedge \left(\mathrm{d}t - \frac{r^2+a^2}{a}\,\mathrm{d}\phi\right). \tag{9}$$

We define the Carter constant as

$$Q := u^\mu \mathcal{K}_{\mu\nu} u^\nu - (\mathcal{L} - a\mathcal{E})^2. \tag{10}$$

Using the constants of motion, the geodesic equations in Kerr spacetime can be written in first order form,

$$\left(\frac{\mathrm{d}r}{\mathrm{d}\lambda}\right)^2 = \left(\mathcal{E}(r^2+a^2) - a\mathcal{L}\right)^2 - \Delta\left(r^2 + (a\mathcal{E} - \mathcal{L})^2 + Q\right) \tag{11a}$$

$$= (1-\mathcal{E}^2)(r_1 - r)(r - r_2)(r - r_3)(r - r_4), \tag{11b}$$

$$\left(\frac{\mathrm{d}z}{\mathrm{d}\lambda}\right)^2 = Q - z^2\left(a^2(1-\mathcal{E}^2)(1-z^2) + \mathcal{L}^2 + Q\right) \tag{11c}$$

$$= (z^2 - z_1^2)\left(a^2(1-\mathcal{E}^2)z^2 - z_2^2\right), \tag{11d}$$

$$\frac{\mathrm{d}t}{\mathrm{d}\lambda} = \frac{r^2+a^2}{\Delta}\left(\mathcal{E}(r^2+a^2) - a\mathcal{L}\right) - a^2\mathcal{E}(1-z^2) + a\mathcal{L}, \tag{11e}$$

and

$$\frac{\mathrm{d}\phi}{\mathrm{d}\lambda} = \frac{a}{\Delta}\left(\mathcal{E}(r^2+a^2) - a\mathcal{L}\right) + \frac{\mathcal{L}}{1-z^2} - a\mathcal{E}, \tag{11f}$$

where we have introduced the Mino(–Carter) time parameter λ [21], defined by

$$\mathrm{d}\tau = \Sigma\,\mathrm{d}\lambda, \tag{12}$$

in order to decouple the radial and polar equations.

In this paper we identify bound orbits in Kerr spacetime by the locations of the radial turning points r_1 and r_2, and the polar turning point z_1. The remaining nodes in equations (11b) and (d) can be found by comparing (11b) and (11d) to (11a) and (11c) and finding the zeroes [19],

$$r_3 = \frac{1}{1-\mathcal{E}^2} - \frac{r_1+r_2}{2} + \sqrt{\left(\frac{r_1+r_2}{2} - \frac{1}{1-\mathcal{E}^2}\right)^2 - \frac{a^2 Q}{r_1 r_2(1-\mathcal{E}^2)}}, \tag{13}$$

$$r_4 = \frac{a^2 Q}{r_1 r_2 r_3(1-\mathcal{E}^2)}, \tag{14}$$

and

$$z_2 = \sqrt{a^2(1-\mathcal{E}^2) + \frac{\mathcal{L}^2}{1-z_1^2}}. \tag{15}$$

Note that our convention for the second polar root z_2 given here (and in equation (11d)) differs from the definitions given in (among others) [19, 22]. The advantage of this convention is that it allows easy evaluation of the $a \to 0$ limit.

The equations for the remaining roots can be inverted to obtain $\mathcal{E}$, $\mathcal{L}$, and Q in terms of r_1, r_2, and z_1 [22]. For convenience (and unity of notation) the explicit expressions are given in appendix A.

2.1. Trajectories

The geodesic equation (11) can be solved as functions of Mino time in closed form using elliptic functions [19, 23–26]. We here repeat the explicit solutions for bound geodesics given by Fujita and Hikida [19], in a much simplified form.

The solutions given in [19] are given in a piecewise manner, making them look more complicated then they are. By applying some of the standard identifies for elliptic functions their solutions can be rewritten in a form that applies at all times. That this should be true can be seen from two simple observations: (1) the solutions should be analytic functions of Mino time, (2) elliptic functions are analytic functions of their arguments. Consequently, if we are given an analytic expression of the solution on some interval, then the analytic extension of that expression should give the solution everywhere.

The solutions of the radial equation (11a) and polar equation (11c) are given by,

$$r(q_r) = \frac{r_3(r_1-r_2)\,\mathsf{sn}^2\left(\frac{\mathsf{K}(k_r)}{\pi}q_r|k_r\right) - r_2(r_1-r_3)}{(r_1-r_2)\,\mathsf{sn}^2\left(\frac{\mathsf{K}(k_r)}{\pi}q_r|k_r\right) - (r_1-r_3)}, \tag{16}$$

and

$$z(q_z) = z_1 \,\mathsf{sn}\left(\mathsf{K}(k_z)\frac{2q_z}{\pi}|k_z\right), \tag{17}$$

where sn is the Jacobi elliptic sine function, K is the complete elliptic integral of the first kind,

$$k_r := \frac{(r_1 - r_2)(r_3 - r_4)}{(r_1 - r_3)(r_2 - r_4)}, \tag{18}$$

and

$$k_z := a^2(1 - \mathcal{E}^2)\frac{z_1^2}{z_2^2}. \tag{19}$$

The solutions are 2π periodic in the radial and polar phases, q_r and q_z, which evolve linearly with Mino time

$$q_r := \Upsilon_r \lambda + q_{r,0}, \tag{20}$$

$$q_z := \Upsilon_z \lambda + q_{z,0}, \tag{21}$$

with 'frequencies'

$$\Upsilon_r = \frac{\pi}{2\mathsf{K}(k_r)}\sqrt{(1 - \mathcal{E}^2)\,(r_1 - r_3)\,(r_2 - r_4)}, \tag{22}$$

and

$$\Upsilon_z = \frac{\pi z_2}{2\mathsf{K}(k_z)}, \tag{23}$$

and where $q_{r,0}$ and $q_{z,0}$ are constants giving the value of q_r and q_z at $\lambda = 0$. Furthermore, we have adopted the convention that $q_r = 0$ corresponds to the periapsis ($r = r_2$), of the radial motion, and $q_z = 0$ corresponds to up going node ($z = 0, z' > 0$) of the polar motion[1]

The solutions for t and ϕ are given by

$$t(q_t, q_r, q_z) = q_t + t_r(q_r) + t_z(q_z), \tag{24}$$

$$t_r(q_r) := \tilde{t}_r\left(\mathsf{am}\left(\mathsf{K}(k_r)\frac{q_r}{\pi}\middle|\, k_r\right)\right) - \frac{\tilde{t}_r(\pi)}{2\pi}q_r, \tag{25}$$

$$t_z(q_z) := \tilde{t}_z\left(\mathsf{am}\left(\mathsf{K}(k_z)\frac{2q_z}{\pi}\middle|\, k_z\right)\right) - \frac{\tilde{t}_z(\pi)}{\pi}q_z, \tag{26}$$

and

$$\phi(q_\phi, q_r, q_z) = q_\phi + \phi_r(q_r) + \phi_z(q_z), \tag{27}$$

$$\phi_r(q_r) := \tilde{\phi}_r\left(\mathsf{am}\left(\mathsf{K}(k_r)\frac{q_r}{\pi}\middle|\, k_r\right)\right) - \frac{\tilde{\phi}_r(\pi)}{2\pi}q_r, \tag{28}$$

$$\phi_z(q_z) := \tilde{\phi}_z\left(\mathsf{am}\left(\mathsf{K}(k_z)\frac{2q_z}{\pi}\middle|\, k_z\right)\right) - \frac{\tilde{\phi}_z(\pi)}{\pi}q_z, \tag{29}$$

[1] Note that this convention for the polar phase q_z differs from the one used by the author in [27] by a shift $\pi/2$.

where am is the amplitude for the Jacobi elliptic functions, and

$$\begin{aligned}\tilde{t}_r(\xi_r) := \frac{\mathcal{E}(r_2-r_3)}{\sqrt{(1-\mathcal{E}^2)(r_1-r_3)(r_2-r_4)}}\Big((4+r_1+r_2+r_3+r_4)\Pi(h_r;\xi_r|k_r)\\ -\frac{4}{r_+-r_-}\left(\frac{r_+(4-a\mathcal{L}/\mathcal{E})-2a^2}{(r_2-r_+)(r_3-r_+)}\Pi(h_+;\xi_r|k_r)-(+\leftrightarrow -)\right)\\ +\frac{(r_1-r_3)(r_2-r_4)}{r_2-r_3}\left(\mathsf{E}(\xi_r|k_r)-h_r\frac{\sin\xi_r\cos\xi_r\sqrt{1-k_r\sin^2\xi_r}}{1-h_r\sin^2\xi_r}\right)\Big),\end{aligned} \tag{30}$$

$$\tilde{t}_z(\xi_z) := -\frac{\mathcal{E}}{1-\mathcal{E}^2}z_2\,\mathsf{E}(\xi_z|k_z), \tag{31}$$

$$\begin{aligned}\tilde{\phi}_r(\xi_r) := -\frac{2a\mathcal{E}(r_2-r_3)}{(r_+-r_-)\sqrt{(1-\mathcal{E}^2)(r_1-r_3)(r_2-r_4)}}\\ \times\left(\frac{2r_+-a\mathcal{L}/\mathcal{E}}{(r_2-r_+)(r_3-r_+)}\Pi(h_+;\xi_r|k_r)-(+\leftrightarrow -)\right),\end{aligned} \tag{32}$$

$$\tilde{\phi}_z(\xi_z) := -\frac{\mathcal{L}}{z_2}\Pi(z_1^2;\xi_z|k_z), \tag{33}$$

where E and Π are elliptic integrals of the second and third kind,

$$h_r := \frac{r_1-r_2}{r_1-r_3}, \tag{34}$$

$$h_\pm := h_r\frac{r_3-r_\pm}{r_2-r_\pm}, \tag{35}$$

and $(+\leftrightarrow -)$ denotes that the preceding term is to be repeated with the $+$ and $-$ symbols in the subscripts exchanged.

The 'phases', q_t and q_ϕ, represent the secularly growing linear parts of the solutions

$$q_t := \Upsilon_t\lambda + q_{t,0}, \tag{36}$$

$$\text{and}\quad q_\phi := \Upsilon_\phi\lambda + q_{\phi,0}, \tag{37}$$

with

$$\Upsilon_t = \tilde{\Upsilon}_{t,r} + \tilde{\Upsilon}_{t,z}, \tag{38}$$

$$\Upsilon_\phi = \tilde{\Upsilon}_{\phi,r} + \tilde{\Upsilon}_{\phi,z}, \tag{39}$$

and

$$\begin{aligned}\tilde{\Upsilon}_{t,r} := (4+a^2)\mathcal{E} + \mathcal{E}\left(\frac{1}{2}\left((4+r_1+r_2+r_3)\,r_3 - r_1r_2 + (r_1-r_3)(r_2-r_4)\frac{\mathsf{E}(k_r)}{\mathsf{K}(k_r)}\right.\right.\\ \left.+(4+r_1+r_2+r_3+r_4)\,(r_2-r_3)\frac{\Pi(h_r|k_r)}{\mathsf{K}(k_r)}\right)+\frac{2}{r_+-r_-}\\ \left.\times\left(\frac{(4-a\mathcal{L}/\mathcal{E})r_+-2a^2}{r_3-r_+}\left(1-\frac{r_2-r_3}{r_2-r_+}\frac{\Pi(h_+|k_r)}{\mathsf{K}(k_r)}\right)-(+\leftrightarrow -)\right)\right),\end{aligned} \tag{40}$$

$$\tilde{\Upsilon}_{t,z} := -a^2\mathcal{E} + \frac{\mathcal{E}Q}{(1-\mathcal{E}^2)z_1^2}\left(1 - \frac{\mathsf{E}(k_z)}{\mathsf{K}(k_z)}\right), \tag{41}$$

$$\tilde{\Upsilon}_{\phi,r} := \frac{a}{r_+ - r_-}\left(\frac{2\mathcal{E}r_+ - a\mathcal{L}}{r_3 - r_+}\left(1 - \frac{r_2 - r_3}{r_2 - r_+}\frac{\Pi(h_+|k_r)}{\mathsf{K}(k_r)}\right) - (+ \leftrightarrow -)\right), \tag{42}$$

$$\tilde{\Upsilon}_{\phi,z} := \frac{\mathcal{L}}{\mathsf{K}(k_z)}\Pi(z_1^2|k_z). \tag{43}$$

One useful aspect of these solutions is that they give explicit closed form expressions for the Mino time frequencies Υ_i. From these one easily obtains the frequencies with respect to coordinate (or Killing) time, Ω_i by taking the ratio with Υ_t,

$$\Omega_i = \frac{\Upsilon_i}{\Upsilon_t}. \tag{44}$$

Moreover, the frequencies with respect to proper time are obtained as

$$\omega_i = \frac{\Upsilon_i}{\Upsilon_\tau}. \tag{45}$$

This requires the average linear increase of proper time with Mino time Υ_τ, which is given in appendix C.

3. Parallel transport

We want to find a tetrad $(e_i)_\mu$ of (co-)vectors that is parallel transported along a generic bound geodesic in Kerr spacetime,

$$u^\alpha \nabla_\alpha (e_i)_\mu = \frac{\mathrm{d}}{\mathrm{d}\tau}(e_i)_\mu - \Gamma^\alpha_{\beta\mu} u^\beta (e_i)_\alpha = 0. \tag{46}$$

In the following tetrad indices are denoted by Roman letters and run from 0 to 3, and spacetime indices are denoted by Greek letters.

In 1983, Marck [16] gave a general procedure for finding such a tetrad given a solution to the geodesic equation in Kerr. We here follow his approach.

A geodesic, by definition, parallel transports its own 4-velocity, u_μ. We can therefore use it as the first leg of our tetrad,

$$(e_0)_\mu := u_\mu = \left(-\mathcal{E}, \frac{1}{\Delta}\frac{\mathrm{d}r}{\mathrm{d}\lambda}, \frac{1}{1-z^2}\frac{\mathrm{d}z}{\mathrm{d}\lambda}, \mathcal{L}\right). \tag{47}$$

Moreover, it follows directly from the defining property of a Killing–Yano tensor, $\nabla_{(\alpha}\mathcal{F}_{\mu)\nu} = 0$, that $\mathcal{F}_{\mu\alpha}u^\alpha$ is also parallel transported along a geodesic. In addition, due to $\mathcal{F}_{\mu\nu}$ being anti-symmetric, this vector is orthogonal to u_μ. This quantity is sometimes interpreted as the total (specific) orbital angular momentum of the geodesic. For us, it serves to construct the last leg

of our tetrad,

$$(e_3)_\mu := \frac{\mathcal{F}_{\mu\alpha}u^\alpha}{\sqrt{\mathcal{K}}} = \frac{1}{\sqrt{\mathcal{K}}}\begin{pmatrix} -a\dfrac{r\frac{\mathrm{d}z}{\mathrm{d}\lambda}+z\frac{\mathrm{d}r}{\mathrm{d}\lambda}}{\Sigma} \\ az\dfrac{(r^2+a^2)\mathcal{E}-a\mathcal{L}}{\Delta} \\ ar\mathcal{E}-\dfrac{r\mathcal{L}}{1-z^2} \\ \dfrac{a^2z(1-z^2)\frac{\mathrm{d}r}{\mathrm{d}\lambda}+r(r^2+a^2)\frac{\mathrm{d}z}{\mathrm{d}\lambda}}{\Sigma} \end{pmatrix}, \tag{48}$$

where

$$\mathcal{K} := u^\alpha \mathcal{K}_{\alpha\beta}u^\beta = Q + (a\mathcal{E}-\mathcal{L})^2. \tag{49}$$

The remaining two tetrad legs must lie in the plane perpendicular to the (co-)vectors $(e_0)_\mu$ and $(e_3)_\mu$. Following Marck [16] we construct an orthonormal basis for this plane,

$$(\tilde{e}_1)_\mu := \frac{1}{\sqrt{\mathcal{K}}}\begin{pmatrix} \dfrac{-\Xi r\frac{\mathrm{d}r}{\mathrm{d}\lambda}+\frac{a^2z}{\Xi}\frac{\mathrm{d}z}{\mathrm{d}\lambda}}{\Sigma} \\ \Xi r\dfrac{(r^2+a^2)\mathcal{E}-a\mathcal{L}}{\Delta} \\ -\dfrac{az}{\Xi}\left(a\mathcal{E}-\dfrac{\mathcal{L}}{1-z^2}\right) \\ a\dfrac{\Xi^2 r(1-z^2)\frac{\mathrm{d}r}{\mathrm{d}\lambda}-z(r^2+a^2)\frac{\mathrm{d}z}{\mathrm{d}\lambda}}{\Xi\Sigma} \end{pmatrix}, \tag{50}$$

and

$$(\tilde{e}_2)_\mu := \begin{pmatrix} \dfrac{\mathcal{E}}{\Xi}-\dfrac{(1-\Xi^2)\left((r^2+a^2)\mathcal{E}-a\mathcal{L}\right)}{\Xi\Sigma} \\ -\dfrac{\Xi}{\Delta}\dfrac{\mathrm{d}r}{\mathrm{d}\lambda} \\ -\dfrac{1}{\Xi(1-z^2)}\dfrac{\mathrm{d}z}{\mathrm{d}\lambda} \\ -\Xi\mathcal{L}-\dfrac{(1-\Xi^2)(r^2+a^2)\left(\mathcal{L}-a(1-z^2)\mathcal{E}\right)}{\Xi\Sigma} \end{pmatrix}, \tag{51}$$

with

$$\Xi := \sqrt{\frac{\mathcal{K}-a^2z^2}{\mathcal{K}+r^2}}. \tag{52}$$

It follows that the remaining two legs of our parallel propagated tetrad must be of the form,

$$(e_1)_\mu := \cos\,\psi(\lambda)(\tilde{e}_1)_\mu + \sin\,\psi(\lambda)(\tilde{e}_2)_\mu, \tag{53}$$

and

$$(e_2)_\mu := -\sin\,\psi(\lambda)(\tilde{e}_1)_\mu + \cos\,\psi(\lambda)(\tilde{e}_2)_\mu. \tag{54}$$

The requirement that $(e_1)_\mu$ and $(e_2)_\mu$ satisfy the parallel transport equation (46), reduces (after some straightforward but tedious algebra) to a single first order differential equation for $\psi(\lambda)$,

$$\frac{\mathrm{d}\psi}{\mathrm{d}\lambda} = \sqrt{\mathcal{K}}\left(\frac{(r^2+a^2)\mathcal{E} - a\mathcal{L}}{\mathcal{K}+r^2} + a\frac{\mathcal{L} - a(1-z^2)\mathcal{E}}{\mathcal{K}-a^2z^2}\right). \tag{55}$$

Since the right-hand side of this equation can be written as the sum of two rational functions, in r and z respectively, it can be solved in terms standard elliptic functions. Following the same general procedure as used in [19] to solve the equations for t and ϕ, we find,

$$\psi(q_\psi, q_r, q_z) = q_\psi + \psi_r(q_r) + \psi_z(q_z) \tag{56}$$

$$\psi_r(q_r) := \tilde{\psi}_r\left(\mathsf{am}\left(\mathsf{K}(k_r)\frac{q_r}{\pi}\middle| k_r\right)\right) - \frac{\tilde{\psi}_r(\pi)}{2\pi}q_r \tag{57}$$

$$\psi_z(q_z) := \tilde{\psi}_z\left(\mathsf{am}\left(\mathsf{K}(k_z)\frac{2q_z}{\pi}\middle| k_z\right)\right) - \frac{\tilde{\psi}_z(\pi)}{\pi}q_z \tag{58}$$

with

$$\begin{aligned}\tilde{\psi}_r(\xi_r) := {} & \frac{2(r_2-r_3)\left((\mathcal{K}-a^2)\mathcal{E}+a\mathcal{L}\right)}{(\mathcal{K}+r_2^2)(\mathcal{K}+r_3^2)\sqrt{(1-\mathcal{E}^2)(r_1-r_3)(r_2-r_4)}} \\ & \times \operatorname{Im}\left((r_2+i\sqrt{\mathcal{K}})(r_3+i\sqrt{\mathcal{K}})\Pi(h_\psi;\xi_r|k_r)\right),\end{aligned} \tag{59}$$

$$\tilde{\psi}_z(\xi_z) := -\frac{(a^2-\mathcal{K})\mathcal{E}-a\mathcal{L}}{\sqrt{\mathcal{K}}z_2}\Pi(\frac{a^2z_1^2}{\mathcal{K}};\xi_z|k_z), \tag{60}$$

and

$$h_\psi := h_r\frac{r_3-i\sqrt{\mathcal{K}}}{r_2-i\sqrt{\mathcal{K}}}. \tag{61}$$

The phases q_r, q_z, and q_ψ are functions of Mino time given by (20), (21), and

$$q_\psi = \Upsilon_\psi\lambda + q_{\psi,0}. \tag{62}$$

Here Υ_ψ is the (Mino time) precession frequency of the tetrad and is given by

$$\Upsilon_\psi = \Upsilon_{\psi,r} + \Upsilon_{\psi,z}, \tag{63}$$

$$\begin{aligned}\Upsilon_{\psi,r} := {} & \frac{\sqrt{\mathcal{K}}\left((r_3^2+a^2)\mathcal{E}-a\mathcal{L}\right)}{r_3^2+\mathcal{K}} + \frac{(r_2-r_3)\left((\mathcal{K}-a^2)\mathcal{E}+a\mathcal{L}\right)}{(r_2^2+\mathcal{K})(r_3^2+\mathcal{K})} \\ & \times \operatorname{Im}\left((r_2+i\sqrt{\mathcal{K}})(r_3+i\sqrt{\mathcal{K}})\frac{\Pi(h_\psi|k_r)}{\mathsf{K}(k_r)}\right),\end{aligned} \tag{64}$$

$$\Upsilon_{\psi,z} := -\mathcal{E}\sqrt{\mathcal{K}} + \frac{(\mathcal{K}-a^2)\mathcal{E}+a\mathcal{L}}{\sqrt{\mathcal{K}}}\frac{\Pi(\frac{a^2z_1^2}{\mathcal{K}}|k_z)}{\mathsf{K}(k_z)}. \tag{65}$$

We thus find a complete closed form analytic solution for the parallel propagation of a tetrad along a generic bound geodesic in Kerr spacetime. A Mathematica implementation of these solutions is included in the KerrGeodesics package of the *Black Hole Perturbation Toolkit* [28].

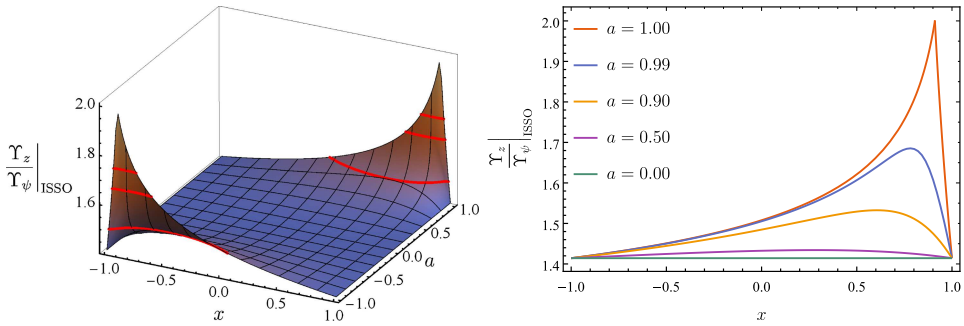

Figure 1. The ratio of the polar frequency Υ_z to the precession frequency Υ_ψ evaluated at the last stable orbit. The left panel shows a 3D plot of this ratio over the full x and a range. The red bands indicate the 3:2, 5:3, and 7:4 resonances. The maximum value of 2 is achieved at $(x, a) = (\pm\sqrt{2(\sqrt{2}-1)}, \pm 1)$. The minimum value of $\sqrt{2}$ is attained when either $a = 0$ or $|x| = 1$. The right panel shows slices of this plot at individual values of the spin a.

4. Application: spin–spin resonances for spherical orbits

One corollary of the analytical solution of parallel transport along a bound geodesic (that was already known from Marck's work [16]), is that parallel transport introduces only one new independent frequency, Υ_ψ, to the three frequencies, $(\Upsilon_r, \Upsilon_z, \Upsilon_\phi)$, which characterize a bound geodesic. Consequently, any time variable effects in the dynamics of a test rigid body around a black hole has a frequency spectrum that consists of integer combinations of Ω_r, Ω_z, Ω_ϕ, and Ω_ψ.

It can occur that for some bound orbit one such combination vanishes. In such a case an effect that is normally oscillatory in nature becomes constant, allowing it to grow secularly over many orbits. Such a situation is known as an (orbital) resonance. The effects of resonances involving the orbital frequencies Ω_r, Ω_z, and Ω_ϕ in extreme mass-ratio inspirals (EMRIs) have been subject of extensive study [29–39]. The appearance of a fourth frequency Ω_ψ allows for the occurrence of new types of resonances.

Having a closed form analytical expression for Υ_ψ (and the other frequencies), is helpful in finding out where and when such resonance can occur. In this section we demonstrate the utility of our expressions by mapping out the locations of resonances between the polar Ω_z frequency and the precession frequency Ω_ψ ($z\psi$-resonances) for inclined circular (a.k.a. spherical) orbits[2].

Note that the coordinate time frequencies Ω_i satisfy a resonance condition if and only if the corresponding Mino time frequencies Υ_i do so as well. Hence, to look for resonances, we can simply look for (low order) rational ratios Υ_z/Υ_ψ.

For resonances involving the Ω_r it is clear that on a trajectory connecting the weak field limit to the last stable orbit Υ_r/Υ_i must pass through all possible resonant ratios between 0 and 1, because by definition $\Upsilon_r = 0$ at the last stable orbit and $\Upsilon_r = \Upsilon_i$ in the weak field. However, for Υ_z/Υ_ψ there is no such guarantee. It is still true that $\Upsilon_z = \Upsilon_\psi$ in the weak field limit. Moreover, we observe empirically that the ratio Υ_z/Υ_ψ increases monotonically with $1/r$ at fixed a and inclination z_1.

[2] This restriction is pure for the sake of ease of presentation. There is no technical obstruction to finding the generic orbit resonances.

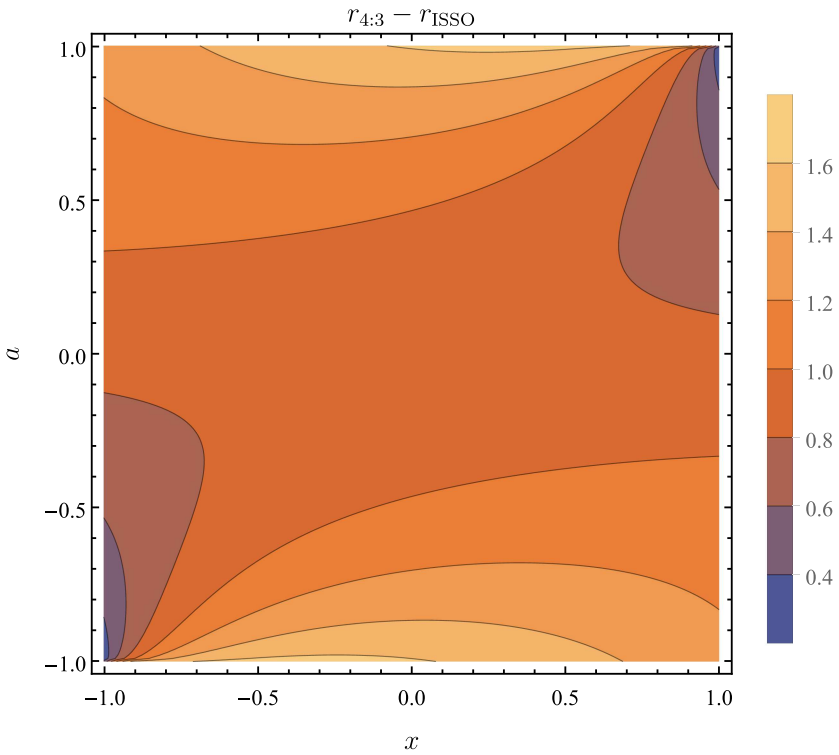

Figure 2. The location of the 4:3 $z\psi$-resonance relative to the location of the innermost stable spherical orbit. This distance is typical of the order of one gravitational radius, meaning the 4:3 $z\psi$-resonance is achieved well before the plunge phase.

Hence, we can determine the range of resonances that can occur for spherical orbits by first determining the ratio Υ_z/Υ_ψ at the innermost stable spherical orbit (ISSO). Figure 1 displays this ratio as a function of the background spin a and the inclination parameter $x := \pm\sqrt{1-z_1^2}$ (with the sign depend on the 'sense' of the orbit, i.e. prograde equatorial orbits have $x = 1$ and retrograde equatorial orbits $x = -1$.) The minimal value of this ratio is attained when $a = 0$ or $|x| = 1$, in which case our analytic expressions tell us that the ratio is exactly $\sqrt{2}$. From figure 1 we also see that the maximum ratio is attained for $|a| = 1$. To find the exact value of this ratio, we note that the location of the ISSO for an extremal Kerr black hole is determined by the relations

$$z_1^2 = \frac{r^2\left(3+3\sqrt{r}-2\sqrt{3+2\sqrt{r}+3r}\right)}{-1+3\sqrt{r}}, \quad r > 1, \tag{66}$$

and

$$r = 1, \quad 0 \leqslant z_1 \leqslant \frac{1}{1+\sqrt{2}}. \tag{67}$$

These relations allow us to evaluate the Υ_z/Υ_ψ on the ISSO in the extremal limit. We find that the maximum is attained when $z_1 = \sqrt{2}-1$—i.e. $x = \text{sign}\ a\sqrt{2(\sqrt{2}-1)}$—the turnover point for the two relations above. At this point the ratio becomes 2.

We thus find that the 2:1 $z\psi$-resonance is not accessible during any quasi-circular inspiral, and the 3:2 $z\psi$-resonance is accessible only in a small part of the parameter space. The lowest order the $z\psi$-resonance that all quasi-circular inspirals must pass through is the 4:3. The location of this resonance relative to the ISSO is shown in figure 2. We see that this resonance happens around $1M$ before the ISSO, which should be well before the plunge phase for most inspirals.

We have here focused purely on the location of the $z\psi$-resonance in the orbital phase space. In order for something to happen at these resonances we also need dynamics that couple the corresponding frequency modes. In EMRIs the first order gravitational self-force is independent of the secondary's spin, and therefore ψ, and hence cannot couple these modes. In [2] it was argued that the Mathisson–Papapetrou–Dixon correction to the orbital dynamics also cannot provide such coupling at linear order in the spin of the smaller object. It is however likely that the first order self-torque (i.e. the linear in mass ratio correction to the dynamics of the secondary spin) will couple at these resonances, as will the second order self-force.

5. Discussion

This paper has provided an explicit closed-form analytic solution for the parallel transport equation along an arbitrary bound geodesic in Kerr spacetime. This result is useful as the zeroth order baseline for studying the dynamics of spinning secondaries and tides in extreme mass-ratio inspirals.

Alternatively, the solutions can be viewed as a providing a set of coordinates to describe EMRI dynamics, which facilitates a two timescale expansion. The phases q_i provide the 'fast' variables of the system varying on the orbital timescale, with all other variables varying on the inspiral timescale. Moreover, the phases q_i are defined in such a way that at zeroth order their derivatives with respect to Mino time are independent of the phases themselves. This means that they provide the necessary starting position to systematically eliminate all variance on the orbital timescale from the perturbed equations of motion using near-identity transformations, allowing efficient integration of the evolution [40].

As an application of our analytical results, we studied the potential occurrence of $z\psi$-resonances in precessing quasi-circular EMRIs. We showed that only resonances with $1 < \Omega_z/\Omega_\psi < 2$ can occur in such inspirals, with resonances with $1 < \Omega_z/\Omega_\psi < \sqrt{2}$ occurring in every quasi-circular inspiral. A more detailed study of resonances involving both generic orbits and arbitrary integer combinations of Ω_r, Ω_z, and Ω_ψ will be left to future work.

Finally, as a bonus feature, we provide an explicit closed form expression for the proper time along a bound geodesic in appendix C. This should be of particular use for studying physics occurring predominantly in the local free falling frame following the geodesics, i.e. the study of tidal disruption of stars on highly eccentric orbits.

Acknowledgments

MvdM is grateful to Chris Kavanagh for help with checking the typesetting of the equations in this work. MvdM was supported by European Union's Horizon 2020 Research and Innovation Programme under Grant Agreement No 705229.

Appendix A. Constants of motion

In order to allow readers to evaluate all formula's in this work without having to trawl through the literature, we reproduce the analytic expressions for $\mathcal{E}$, $\mathcal{L}$, and Q in terms of r_1, r_2, and z_1 first given by [22].

$$\mathcal{E} = \sqrt{\frac{\kappa\rho + 2\epsilon\sigma - 2a\sqrt{\frac{\sigma}{a^2}\left(\sigma\epsilon^2 + \rho\epsilon\kappa - \eta\kappa^2\right)}}{\rho^2 + 4\eta\sigma}}, \tag{A.1}$$

$$\mathcal{L} = -\frac{g(r_2)\mathcal{E} - \sqrt{(g(r_2)^2 + h(r_2)f(r_2))\mathcal{E}^2 - h(r_2)d(r_2)}}{h(r_2)}, \tag{A.2}$$

and

$$Q = z_1^2\left(a^2(1-\mathcal{E}^2) + \frac{\mathcal{L}^2}{1-z_1^2}\right) \tag{A.3}$$

with

$$\kappa := d(r_2)h(r_1) - (r_1 \leftrightarrow r_2), \tag{A.4}$$

$$\epsilon := d(r_2)g(r_1) - (r_1 \leftrightarrow r_2), \tag{A.5}$$

$$\rho := f(r_2)h(r_1) - (r_1 \leftrightarrow r_2), \tag{A.6}$$

$$\eta := f(r_2)g(r_1) - (r_1 \leftrightarrow r_2), \tag{A.7}$$

$$\sigma := g(r_2)h(r_1) - (r_1 \leftrightarrow r_2), \tag{A.8}$$

and

$$d(r) := \Delta(r)\left(r^2 + a^2 z_1^2\right), \tag{A.9}$$

$$f(r) := r^4 + a^2\left(r(r+2) + z_1^2\Delta(r)\right), \tag{A.10}$$

$$g(r) := 2ar, \tag{A.11}$$

and

$$h(r) := r(r-2) + \frac{z_1^2\Delta(r)}{1-z_1^2}. \tag{A.12}$$

Appendix B. Elliptic functions

We here give an overview of the definitions of the elliptic functions used throughout this paper. We generally follow the some notational conventions as Mathematica.

Function	Definition	Description
$\mathsf{F}(\xi\|k)$	$\int_0^\xi \frac{1}{\sqrt{1-k\sin^2\chi}}\,\mathrm{d}\chi$	Elliptic integral of the first kind
$\mathsf{K}(k)$	$\mathsf{F}(\frac{\pi}{2}\|k)$	Complete elliptic integral of the first kind
$\mathsf{E}(\xi\|k)$	$\int_0^\xi \sqrt{1-k\sin^2\chi}\,\mathrm{d}\chi$	Elliptic integral of the second kind
$\mathsf{E}(k)$	$\mathsf{E}(\frac{\pi}{2}\|k)$	Complete elliptic integral of the second kind
$\Pi(h;\xi\|k)$	$\int_0^\xi \frac{1}{(1-h\sin^2\chi)\sqrt{1-k\sin^2\chi}}\,\mathrm{d}\chi$	Elliptic integral of the third kind
$\Pi(h\|k)$	$\Pi(h;\frac{\pi}{2}\|k)$	Complete elliptic integral of the third kind
$\mathsf{am}(u\|k)$	$u=\mathsf{F}\left(\mathsf{am}(u\|k)\|k\right)$	Jacobi amplitude
$\mathsf{sn}(u\|k)$	$\sin(\mathsf{am}(u\|k))$	Jacobi elliptic sine

Appendix C. Proper time

The explicit closed form solutions for bound geodesics and parallel transport along them are given as functions of Mino time. However, for some applications it is useful to know the proper time along the orbit as well, e.g. when constructing explicit local Fermi–Walker coordinates around the orbit.

The relation between Mino time and proper time is given by

$$\frac{\mathrm{d}\tau}{\mathrm{d}\lambda} = \Sigma = r^2 + a^2 z^2. \tag{C.1}$$

This equation can be solved through the same means as used to solve the equations for t, ϕ, and ψ. We give the explicit solution here,

$$\tau(q_\tau, q_r, q_z) = q_\tau + \tau_r(q_r) + \tau_z(q_z), \tag{C.2}$$

$$\tau_r(q_r) := \tilde{\tau}_r\left(\mathsf{am}\left(\mathsf{K}(k_r)\frac{q_r}{\pi}\middle|\, k_r\right)\right) - \frac{\tilde{\tau}_r(\pi)}{2\pi}q_r, \tag{C.3}$$

$$\tau_z(q_z) := \tilde{\tau}_z\left(\mathsf{am}\left(\mathsf{K}(k_z)\frac{2q_z}{\pi}\middle|\, k_z\right)\right) - \frac{\tilde{\tau}_z(\pi)}{\pi}q_z \tag{C.4}$$

with

$$\begin{aligned}\tilde{\tau}_r(\xi_r) := \frac{1}{\sqrt{(1-\mathcal{E}^2)(r_1-r_3)(r_2-r_4)}}\Bigg(&((r_1+r_2+r_3)r_3 - r_1 r_2)\,\mathsf{F}(\xi_r|k_r)\\ &+ (r_1-r_3)(r_2-r_4)\mathsf{E}(\xi_r|k_r) + (r_2-r_3)(r_1+r_2+r_3+r_4)\Pi(h_r;\xi_r|k_r)\\ &-\frac{h_r(r_1-r_3)(r_2-r_4)\sin\xi_r\cos\xi_r\sqrt{1-k_r\sin^2\xi_r}}{1-h_r\sin^2\xi_r}\Bigg),\end{aligned} \tag{C.5}$$

and

$$\tilde{\tau}_z(\xi_z) := \frac{z_2}{(1-\mathcal{E}^2)}\left(\mathsf{F}(\xi_z|k_z) - \mathsf{E}(\xi_z|k_z)\right). \tag{C.6}$$

The secular part q_τ evolves linearly with λ,

$$q_\tau = \Upsilon_\tau \lambda + q_{\tau,0}, \tag{C.7}$$

with 'frequency'

$$\Upsilon_\tau = \tilde{\Upsilon}_{\tau,r} + \tilde{\Upsilon}_{\tau,z}, \tag{C.8}$$

$$\tilde{\Upsilon}_{\tau,r} := \frac{(r_1+r_2+r_3)r_3 - r_1 r_2}{2} + (r_1-r_3)(r_2-r_4)\frac{\mathsf{E}(k_r)}{2\mathsf{K}(k_r)} + (r_1+r_2+r_3+r_4)(r_2-r_3)\frac{\Pi(h_r|k_r)}{2\mathsf{K}(k_r)}, \tag{C.9}$$

and

$$\tilde{\Upsilon}_{\tau,z} := \frac{z_2^2}{1-\mathcal{E}^2}\left(1 - \frac{\mathsf{E}(k_z)}{\mathsf{K}(k_z)}\right). \tag{C.10}$$

This explicit analytic expression for the Υ_τ also allows for the calculation of the proper time frequencies ω_{i} through

$$\omega_i = \frac{\Upsilon_i}{\Upsilon_\tau}. \tag{C.11}$$

ORCID iDs

Maarten van de Meent https://orcid.org/0000-0002-0242-2464

References

[1] Barack L and Adam P 2019 Self-force and radiation reaction in general relativity *Rept. Prog. Phys.* **82** 016904
[2] Ruangsri U, Vigeland S J and Hughes S A 2016 Gyroscopes orbiting black holes: a frequency-domain approach to precession and spin–curvature coupling for spinning bodies on generic Kerr orbits *Phys. Rev.* D **94** 044008
[3] Warburton N, Osburn T and Evans C R 2017 Evolution of small-mass-ratio binaries with a spinning secondary *Phys. Rev.* D **96** 084057
[4] Witzany V 2019 Spin-perturbed orbits near black holes (arXiv:1903.03649 [gr-qc])
[5] Witzany V 2019 Hamilton–Jacobi equation for spinning particles near black holes *Phys. Rev.* D **100** 104030
[6] Dolan S R, Warburton N, Harte A I, Le Tiec A, Wardell B *et al* 2014 Gravitational self-torque and spin precession in compact binaries *Phys. Rev.* D **89** 064011
[7] Bini D and Damour T 2014 Two-body gravitational spin–orbit interaction at linear order in the mass ratio *Phys. Rev.* D **90** 024039
[8] Shah A G and Pound A 2015 Linear-in-mass-ratio contribution to spin precession and tidal invariants in Schwarzschild spacetime at very high post-Newtonian order *Phys. Rev.* D **91** 124022
[9] Bini D and Damour T 2015 Analytic determination of high-order post-Newtonian self-force contributions to gravitational spin precession *Phys. Rev.* D **91** 064064
[10] Kavanagh C, Ottewill A C and Wardell B 2015 Analytical high-order post-Newtonian expansions for extreme mass ratio binaries *Phys. Rev.* D **92** 084025
[11] Akcay S, Dempsey D and Dolan S R 2017 Spin–orbit precession for eccentric black hole binaries at first order in the mass ratio *Class. Quantum Grav.* **34** 084001
[12] Kavanagh C, Bini D, Damour T, Hopper S, Ottewill A C and Wardell B 2017 Spin–orbit precession along eccentric orbits for extreme mass ratio black hole binaries and its effective-one-body transcription *Phys. Rev.* D **96** 064012

[13] Bini D, Damour T and Geralico A 2018 Spin–orbit precession along eccentric orbits: improving the knowledge of self-force corrections and of their effective-one-body counterparts *Phys. Rev.* D **97** 104046
[14] Bini D, Damour T, Geralico A, Kavanagh C and van de Meent M 2018 Gravitational self-force corrections to gyroscope precession along circular orbits in the Kerr spacetime *Phys. Rev.* D **98** 104062
[15] Akcay S 2017 Self-force correction to geodetic spin precession in Kerr spacetime *Phys. Rev.* D **96** 044024
[16] Marck J 1983 Solution to the equations of parallel transport in Kerr geometry; tidal tensor *Proc. R. Soc.* A **385** 431–8
[17] Bini D, Geralico A and Jantzen R T 2017 Gyroscope precession along general timelike geodesics in a Kerr black hole spacetime *Phys. Rev.* D **95** 124022
[18] Bini D, Geralico A and Jantzen R T 2019 Black hole geodesic parallel transport and the Marck reduction procedure *Phys. Rev.* D **99** 064041
[19] Fujita R and Hikida W 2009 Analytical solutions of bound timelike geodesic orbits in Kerr spacetime *Class. Quantum Grav.* **26** 135002
[20] Carter B 1968 Global structure of the Kerr family of gravitational fields *Phys. Rev.* **174** 1559–71
[21] Mino Y 2003 Perturbative approach to an orbital evolution around a supermassive black hole *Phys. Rev.* D **67** 084027
[22] Schmidt W 2002 Celestial mechanics in Kerr space-time *Class. Quantum Grav.* **19** 2743
[23] Kraniotis G V 2004 Precise relativistic orbits in Kerr space-time with a cosmological constant *Class. Quantum Grav.* **21** 4743–69
[24] Hackmann E and Lammerzahl C 2008 Geodesic equation in Schwarzschild-(anti-)de Sitter space-times: analytical solutions and applications *Phys. Rev.* D **78** 024035
[25] Hackmann E 2010 Geodesic equations in black hole space-times with cosmological constant *PhD Thesis* Bremen U
[26] Hackmann E, Lammerzahl C, Kagramanova V and Kunz J 2010 Analytical solution of the geodesic equation in Kerr-(anti) de Sitter space-times *Phys. Rev.* D **81** 044020
[27] van de Meent M 2018 Gravitational self-force on generic bound geodesics in Kerr spacetime *Phys. Rev.* D **97** 104033
[28] Black hole perturbation toolkit bhptoolkit.org
[29] Flanagan E E and Hinderer T 2012 Transient resonances in the inspirals of point particles into black holes *Phys. Rev. Lett.* **109** 071102
[30] Flanagan E E, Hughes S A and Ruangsri U 2014 Resonantly enhanced and diminished strong-field gravitational-wave fluxes *Phys. Rev.* D **89** 084028
[31] Ruangsri U and Hughes S A 2014 A census of transient orbital resonances encountered during binary inspiral *Phys. Rev.* D **89** 084036
[32] Brink J, Geyer M and Hinderer T 2015 Astrophysics of resonant orbits in the Kerr metric *Phys. Rev.* D **91** 083001
[33] Gair J, Yunes N and Bender C M 2012 Resonances in extreme mass-ratio inspirals: asymptotic and hyperasymptotic analysis *J. Math. Phys.* **53** 032503
[34] Berry C P L, Cole R H, Cañizares P and Gair J R 2016 Importance of transient resonances in extreme-mass-ratio inspirals *Phys. Rev.* D **94** 124042
[35] Mihaylov D P and Gair J R 2017 Transition of EMRIs through resonance: corrections to higher order in the on-resonance flux modification *J. Math. Phys.* **58** 112501
[36] van de Meent M 2014 Conditions for sustained orbital resonances in extreme mass ratio inspirals *Phys. Rev.* D **89** 084033
[37] van de Meent M 2014 Resonantly enhanced kicks from equatorial small mass-ratio inspirals *Phys. Rev.* D **90** 044027
[38] Hirata C M 2011 Resonant recoil in extreme mass ratio binary black hole mergers *Phys. Rev.* D **83** 104024
[39] Bonga B, Yang H and Hughes S A 2019 Tidal resonance in extreme mass-ratio inspirals *Phys. Rev. Lett.* **123** 101103
[40] van de Meent M and Warburton N 2018 Fast self-forced inspirals *Class. Quantum Grav.* **35** 144003